Organotransition-Metal Metallacarboranes. 19.[1] Indenyliron(II) and -iron(III) Complexes and Related Species. $\eta^6 \rightarrow \eta^5$ Haptotropic Rearrangement, Electrochemistry, and Polyhedral Expansion of (Arene)Fe($Et_2C_2B_4H_4$) Clusters

Achim Fessenbecker,[2a,b] Martin Stephan,[2a,b] Russell N. Grimes,*[,2a] Hans Pritzkow,[2b] Ulrich Zenneck,[2b] and Walter Siebert*[,2b]

Contribution from the Department of Chemistry, University of Virginia, Charlottesville, Virginia 22901, and Anorganische-Chemisches Institut der Universität, D-6900 Heidelberg, Federal Republic of Germany. *Received October 25, 1990*

Abstract: Thermal displacement of the cyclooctatriene ligand in (η^6-C_8H_{10})Fe^{II}($Et_2C_2B_4H_4$) by indene at 180 °C afforded orange air-stable (η^6-C_9H_8)Fe^{II}($Et_2C_2B_4H_4$) (**1**) in high yield together with a minor product (**2**), which is evidently a dimer of **1**. The η^6-coordination of indene to iron in **1** was confirmed by X-ray diffraction. Treatment of **1** with tetramethylethylenediamine (TMEDA) gave the yellow decapitated product (η^6-C_9H_8)Fe^{II}($Et_2C_2B_3H_5$) (**3**). Deprotonation of **1** at −78 °C gave a violet anionic intermediate; reaction of that species with dry HCl at −78 °C regenerated **1**. However, when the anion was warmed to 0 °C or higher, proton NMR data indicated that a haptotropic rearrangement occurred to produce the (η^5-C_9H_7)Fe($Et_2C_2B_4H_4$)$^-$ anion **4**$^-$. Treatment of the latter species with HCl·Et_2O gave the Fe-protonated complex (η^5-C_9H_7)FeH($Et_2C_2B_4H_4$) (**5**), which on reaction with NaH regenerated **4**$^-$. Exposure of **4**$^-$ or **5** to oxygen gave magenta, paramagnetic (η^5-C_9H_7)Fe^{III}($Et_2C_2B_4H_4$) (**4**), whose ESR spectrum supports the assignment of an Fe(III) oxidation state; reduction of **4** with potassium metal afforded **4**$^-$ quantitatively. The reaction of the **4**$^-$ anion with LiCp*/$NiBr_2$, and with the cobalt–diborole complex CpCo($Et_2MeC_3B_2Et_2$)$^-$ and $NiBr_2$, generated, respectively, the compounds (η^5-C_9H_7)Fe($Et_2C_2B_4H_4$)NiCp* (**6**) and (η^5-C_9H_7)Fe($Et_2C_2B_4H_4$)Ni($Et_2MeC_3B_2Et_2$)CoCp (**7**). An X-ray diffraction study of **6** established that these species incorporate eight-vertex $FeNiC_2B_4$ clusters, representing the first clear examples of cage expansion of a seven-vertex metallacarborane via metal insertion. In **7**, the nickel atom also participates in a seven-vertex $NiCoC_3B_2$ cluster. In an analogous reaction, Cp*Fe($Et_2C_2B_4H_4$)$^-$ (**8**$^-$, a C_5Me_5 counterpart of **4**$^-$) and LiCp*/$NiBr_2$ gave Cp*Fe($Et_2C_2B_4H_4$)NiCp* (**9**), which was assigned an $FeNiC_2B_4$ cluster geometry corresponding to that of **6**. A similar reaction of **8**$^-$ with the cobalt–diborole complex CpCo($Et_2HC_3B_2Me_2$)$^-$ produced Cp*Fe($Et_2C_2B_4H_4$)Ni($Et_2HC_3B_2Me_2$)CoCp (**10**), whose proposed structure is analogous to that of **7**. The new compounds were isolated via column and/or plate chromatography on silica and characterized from their ^1H, ^{11}B, and (in some cases) ^{13}C NMR spectra; infrared and mass spectra; ESR spectra on **4**; and crystallographic studies on **1** and **6**. In addition, cyclic voltammetry was conducted on the compounds **1**, **3**, **4**, **5**, and **7**. The electrochemical behavior of most species examined was complex, with oxidation and/or reduction leading in several cases to chemical reactions whose products generate further signals during cyclic voltammetry. Crystal data for **1**: mol wt 301.4; space group $P2_1/c$; $Z = 4$; $a = 8.267$ (3), $b = 14.459$ (6), $c = 13.512$ (5) Å; $\beta = 103.04$ (3)°; $V = 1574$ Å^3; $R = 0.041$ for 2081 reflections having $F_o^2 > 2.0\sigma(F_o^2)$. Crystal data for **6**: mol wt 494.3; space group $P2_1/a$; $Z = 4$; $a = 14.529$ (8), $b = 8.507$ (5), $c = 20.374$ (12) Å; $\beta = 93.09$ (4)°; $V = 2514$ Å^3; $R = 0.038$ for 3754 reflections having $F_o^2 > 2.0\sigma(F_o^2)$.

Introduction

Metallacarboranes of the type $LM(R_2C_2B_4H_4)$, in which L is $C_5H_5^-$, $C_5Me_5^-$, or an arene, and M is a transition metal, are, of course, MC_2B_4 clusters, but it is equally valid to describe them as mixed-ligand complexes in which the metal cation is sandwiched between aromatic hydrocarbon and carborane ($R_2C_2B_4H_4^{2-}$) ligands. This dual nature is reflected in published studies of such species, which tend to focus either on their cluster character (involving phenomena such as cage rearrangement, cage opening, and metal insertion)[3] or on their organometallic properties, in which attention centers primarily on the metal–hydrocarbon ligand group.[4] As the ability of $R_2C_2B_4H_4^{2-}$ units to stabilize organometallic species has become increasingly apparent, our interest in this latter aspect has grown accordingly.

In this paper we report on an investigation of (indenyl)Fe($Et_2C_2B_4H_4$) complexes, which continues our cooperative study of metallaboron chemistry involving carborane (C_2B_3, C_2B_4) and diborole (C_3B_2) ligands,[5-7] and which has led to significant findings involving both the boron cluster and transition-metal organometallic properties of these molecules. The indenylferracarborane system was selected for study partly as an extension of earlier work on (arene)Fe($Et_2C_2B_4H_4$) species,[8] but also with the intention of preparing bimetallic indenyl-bridged trilevel complexes of the formula $LM(\eta^5,\eta^6$-indenyl)Fe($Et_2C_2B_4H_4$). As it turned out, no such complexes were obtained, but we were rewarded with some surprising chemistry in both the carborane and organometallic areas.

Results and Discussion

Synthesis of Indenylferracarboranes. The complex (η^6-C_9H_8)Fe($Et_2C_2B_4H_4$) (**1**) was obtained from (η^6-C_8H_{10})Fe($Et_2C_2B_4H_4$) via thermal displacement of cyclooctatriene by indene

(1) Part 18: Davis, J. H., Jr.; Benvenuto, M.; Grimes, R. N. *Inorg. Chem.*, in press.
(2) (a) University of Virginia. (b) University of Heidelberg.
(3) An overview of these topics is given by: Grimes, R. N. In *Comprehensive Organometallic Chemistry*; Wilkinson, G., Stone, F. G. A.; Abel, E., Eds.; Pergamon Press: Oxford, England, 1982; Chapter 5.5.
(4) Reviews: (a) Grimes, R. N. *Pure Appl. Chem.* **1987**, *59*, 847. (b) Grimes, R. N. Cyclocarborane-Stabilized Multidecker/Multicluster Sandwich Compounds and Linked Molecular Systems. In *Electron-Deficient Boron and Carbon Clusters*; Olah, G. A., Wade, K., Williams, R. E., Eds.; John Wiley and Sons: New York, 1991. Recent papers: (c) Davis, J. H., Jr.; Attwood, M. D.; Grimes, R. N. *Organometallics* **1990**, *9*, 1171. (d) Attwood, M. D.; Davis, J. H., Jr.; Grimes, R. N. *Organometallics* **1990**, *9*, 1177. (e) Davis, J. H., Jr.; Sinn, E.; Grimes, R. N. *J. Am. Chem. Soc.* **1989**, *111*, 4776. (f) Davis, J. H., Jr.; Sinn, E.; Grimes, R. N. *J. Am. Chem. Soc.* **1989**, *111*, 4784.
(5) Attwood, M. A.; Fonda, K. K.; Grimes, R. N.; Brodt, G.; Hu, D.; Zenneck, U.; Siebert, W. *Organometallics* **1989**, *8*, 1300.
(6) Fessenbecker, A.; Attwood, M. D.; Bryan, R. F.; Grimes, R. N.; Woode, M. K.; Stephan, M.; Zenneck, U.; Siebert, W. *Inorg. Chem.* **1990**, *29*, 5157.
(7) Fessenbecker, A.; Attwood, M. D.; Grimes, R. N.; Stephan, M.; Pritzkow, H.; Zenneck, U.; Siebert, W. *Inorg. Chem.* **1990**, *29*, 5164.
(8) (a) Swisher, R. G.; Sinn, E.; Grimes, R. N. *Organometallics* **1983**, *2*, 506. (b) Swisher, R. G.; Butcher, R. J.; Sinn, E.; Grimes, R. N. *Organometallics* **1985**, *4*, 882. (c) Swisher, R. G.; Sinn, E.; Grimes, R. N. *Organometallics* **1985**, *4*, 890. (d) Swisher, R. G.; Sinn, E.; Grimes, R. N. *Organometallics* **1985**, *4*, 896. (e) Spencer, J. T.; Grimes, R. N. *Organometallics* **1987**, *6*, 323. (f) Spencer, J. T.; Grimes, R. N. *Organometallics* **1987**, *6*, 328.

0002-7863/91/1513-3061$02.50/0

Table I. 115.8-MHz ^{11}B FT NMR Data

compound	δ (J_{BH}, Hz)[a-c]	rel areas
$(\eta^6\text{-}C_9H_8)Fe(Et_2C_2B_4H_4)$ (**1**)	7.7 (142), 4.3 (173), 2.2 (176), 0.8 (161)	1:1:1:1
$[(C_9H_7)Fe(Et_2C_2B_4H_4)]_2$ (**2**)	8.7 (112), 5.3, 2.8, 1.4	1:1:1:1
$(\eta^6\text{-}C_9H_8)Fe(Et_2C_2B_3H_5)$ (**3**)	3.1 (144), 0.5, 0.1	1:1:1
$(\eta^5\text{-}C_9H_7)FeH(Et_2C_2B_4H_4)$ (**5**)	−4.7 (162), −8.1 (156), −20.3 (147)	1:2:1
$(\eta^5\text{-}C_9H_7)Fe(Et_2C_2B_4H_4)Ni(C_5Me_5)$ (**6**)	117.2 (151), 28.7 (157), −7.3 (147)	1:1:2
$(\eta^5\text{-}C_9H_7)Fe(Et_2C_2B_4H_4)Ni(Et_2MeC_3B_2Et_2)CoCp$ (**7**)	118.7 (135), 28.2,[d] 25.9 (162), 13.3,[d] −5.9 (138)	1:1:1:1:2
$(C_5Me_5)Fe(Et_2C_2B_4H_4)Ni(C_5Me_5)$ (**9**)	119.1 (139), 26.7 (159), −7.9 (138)	1:1:2
$(C_5Me_5)Fe(Et_2C_2B_4H_4)Ni(Et_2HC_3B_2Me_2)CoCp$ (**10**)	118.9 (138), 31.3,[d] 25.8 (158), 12.8,[d] −6.2 (142)	1:1:1:1:2

[a] Shifts relative to $BF_3{\cdot}OEt_2$, positive values downfield. [b] *n*-Hexane solution. [c] H–B coupling constant in hertz is given in parentheses, when resolved. [d] Diborolyl ring B–alkyl singlet resonance.

Table II. 300-MHz ^1H FT NMR Data

compd	δ[a-c]
1	6.70 (m, indene C_5 ring CHs), [5.88 d, 5.56 d] (indene[d] H5, H11), 5.31 (m, indene H4, H12), 3.37 (dd, indene C_5 ring CH_2), 2.45 (m, ethyl CH_2), 2.21 (ethyl CH_2), 1.20 (t, CH_3), 1.13 (t, CH_3)
2	6.59 (d), 6.48 (s), 6.37 (d), 5.83 (d), 5.44 (m), 5.38 (d), 5.28 (m), 5.20 (m), 5.10 (t), 4.29 (s), 2.46 (m), 2.23 (m), 1.19 (t), 1.18 (t), 1.16 (t), 1.13 (t)
3	6.60 (s, indene C_5 ring CHs), [5.73 d, 5.53 d] (indene[d] H5, H11), [5.21 t, 5.13 t] (indene H4, H12), 3.31 (q, indene C_5 ring CH_2), 1.93 (m), 1.08 (t), 1.05 (t), −6.6 (s[e])
4	38.0, 30.4, 10.1, 1.5, −2.1, −7.2, −8.2, −39
5	[7.44 m, 7.16 m] (indenyl C_6 ring), [4.94 s, br, 4.24 s, br] (indenyl C_5 ring), 2.31 (m, CH_2), 2.06 (m, CH_2), 1.14 (t, CH_3), −11.15 (s, Fe–H)
6	[7.0 m, 6.9 m] (indenyl C_6 ring), [6.02 t, 5.07 d] (indenyl C_5 ring), 2.21 (m, CH_2), 1.66 (s, CH_3), 1.66 (m, CH_2), 0.93 (t, CH_3)
7[f]	6.48 (m, indenyl C_6 ring), [5.64 t, 4.75 d] (indenyl C_5 ring), 4.14 (s, C_5H_5 ring), 2.42 (dq, CH_2), 2.09 (s, diborole C-CH_3), 2.02 (CH_2), 1.28 (t, CH_3), 0.98 (t, CH_3), 0.82 (t, CH_3)
9	2.84 (m, CH_2), 2.12 (m, CH_2), 1.70 (s, C_5Me_5), 1.56 (s, C_5Me_5), 1.23 (t, CH_3)
10	4.45 (s, C_5H_5), 3.26 (s, diborole CH), 2.52 (m, CH_2), 2.24 (m, CH_2), 1.85 (CH_2), 1.45 (s, C_6Me_5), 1.23 (t, ethyl CH_3), 1.12 (t, ethyl CH_3), 0.67 (s, B-CH_3)

[a] $CDCl_3$ solution except where otherwise indicated. [b] Shifts relative to $(CH_3)_4Si$. Integrated peak areas in all cases are consistent with the assignments given. Legend: m, multiplet; s, singlet; d, doublet; dd, doublet of doublets; t, triplet; q, quartet. [c] $B\text{–}H_{terminal}$ resources are broad quartets and mostly obscured by other signals. [d] Atom numbering is taken from X-ray structure determination (Figure 1). [e] B–H–B proton resonance. [f] C_6D_6 solution.

Table III. Infrared Absorptions (cm^{-1}, Neat Films on KBr Plates)[a,b]

compd	absorptions
1	2967 s, 2930 s, 2910 m, 2525 vs, 2339 m, 2336 m, 1700 m, 1653 m, 1539 m, 1436 m, 1419 w, 1387 w, 1336 m, 875 w, 746 w, 734 w, 667 w
2	2965 s, 2927 s, 2521 s, 2491 s, 1426 m, 1416 m, 1374 m, 1333 m, 1184 w, 1172 w, 1120 w, 1070 m, 980 w, 885 m, 861 m, 823 m, 800 m, 746 m, 710 m
3	2961 s, 2924 m, 2901 m, 2858 m, 2842 m, 2538 m, 2481 vs, 2361 m, 2336 vs, 1868 m, 1381 m, 928 m, 839 m, 777 m, 735 m, 667 m, 663 m
4	2965 s, 2929 s, 2872 m, 2855 m, 2544 s, 1444 m, 1376 m, 1336 w, 1260 w, 1207 w, 1093 w, 1029 m, 900 w, 836 w, 797 w, 754 m
5	2966 s, 2929 s, 2874 s, 2872 s, 2854 s, 2852 s, 2561 s, 1449 s, 1113 m, 1095 m, 1093 m, 1088 m, 1084 w, 1077 w, 1070 w, 1053 m, 1030 m, 746 w
6	2957 s, 2923 s, 2871 s, 2853 s, 2499 m, 2470 m, 1376 m, 1093 w, 1078 w, 1074 w, 1039 w, 1030 w, 910 m, 817 w, 777 w, 743 m
7	2960 m, 2924 s, 2881 m, 2869 m, 2866 m, 2851 m, 2515 w, 2361 s, 239 s, 1273 w, 1114 m, 1032 m, 918 w, 821 s, 769 w, 679 s
9	2967 s, 2914 s, 2862 m, 2857 m, 2527 s, 2478 s, 1375 s, 1275 w, 1150 w, 1060 w, 1027 m, 926 w, 853 w, 793 w, 741 w
10	3067 m, 3043 m, 2964 m, 2928 m, 2504 s, 2348 s, 2282 s, 1363 m, 1305 m, 1242 w, 1203 w, 1002 w, 894 w, 882 w, 806 m

[a] Microcrystalline films obtained by evaporation of solutions. [b] Legend: vs, very strong; s, strong; m, medium; w, weak; sh, shoulder; br, broad.

in a sealed tube. Chromatography on silica in *n*-hexane gave **1** in 80% isolated yield (Scheme I) as bright yellow-orange crystals, which were characterized from the mass spectrum, ^1H, ^{11}B, and ^{13}C NMR spectra, infrared spectrum (Tables I–III and Experimental Section), and X-ray diffraction data (Tables IV and V), which confirmed the geometry shown. A minor product (**2**), isolated in 3–5% yield, was characterized as a dimer having the composition $[(C_9H_7)Fe(Et_2C_2B_4H_4)]_2$.

The proton NMR data on **1** indicate that the iron–indene bonding in $CDCl_3$ solution is the same as that in the solid state, since the resonances of the C_6 ring protons are shifted to higher field compared to those in free indene, indicating coordination of the metal to the C_6 ring. The ^{11}B NMR spectrum exhibits four clearly resolved resonances in a 1:1:1:1 pattern, reflecting the inequivalence of B4 and B6, which arises from the presence of the indenyl ligand. In the ^{13}C spectrum, peaks are observed for each of the 15 inequivalent carbon nuclei in the molecule, which is chiral and exists as a racemate in both the solution and solid.

The solid-state structure of **1** (Figure 1) consists of a closo seven-vertex FeC_2B_4 cage with no unusual interatomic distances in comparison to other FeC_2B_4 clusters.[8a-d,9] The iron atom is

Table IV. Experimental X-ray Diffraction Parameters and Crystal Data

	1	**6**
space group	$P2_1/c$	$P2_1/a$
a, Å	8.267 (3)	14.529 (8)
b, Å	14.459 (6)	8.507 (5)
c, Å	13.512 (5)	20.374 (12)
β, deg	103.04 (3)	93.09 (4)
V, Å^3	1574	2514
Z	4	4
μ, cm^{-1} (Mo Kα)	8.87	12.71
transmission factors	0.51–0.72	0.46–0.58
λ, Å	0.7107	0.7107
D(calcd), g cm^{-3}	1.272	1.306
crystal size, mm	0.3 × 0.4 × 0.7	0.5 × 0.6 × 0.7
2θ range, deg	3–50	3–55
no. of reflectns measd	2889	6228
no. of reflectns obsd	2081	3754
R	0.041	0.038
R_w	0.050	0.045
largest peak in final diff map, e/Å^3	0.3	0.3

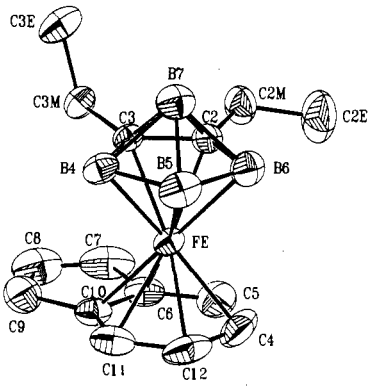

Figure 1. Molecular structure of **1**, with hydrogen atoms omitted.

Scheme I

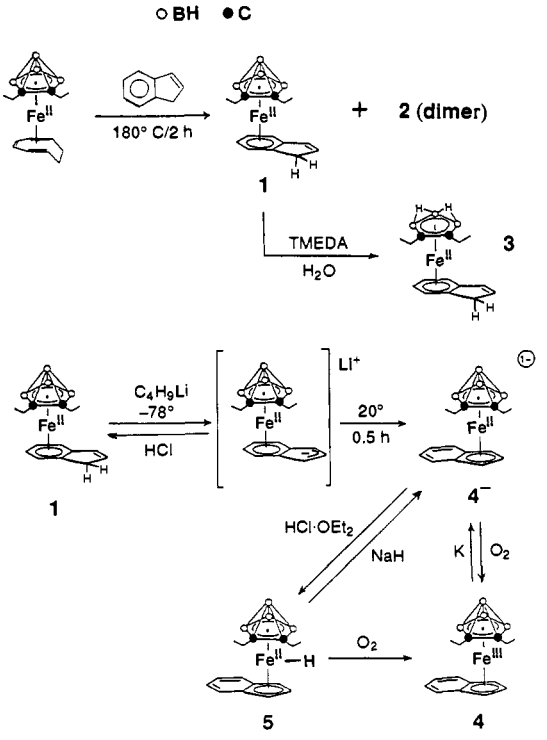

nearly equidistant from the C_6 ring carbons, and the C_6 and C_2B_3 rings are nearly parallel, with a dihedral angle of 2.8°. The C_5 ring is, however, disordered with the C=C bond partially present at both C7–C8 and C8–C9, whose distances (1.383 (8) and 1.375 (9) Å, respectively) are between those of normal C–C single and double bonds. The geometry of the dimer **2** has not been assigned in detail, but comparison of its ^{11}B and ^1H NMR spectra with those of **1** indicates that, while the FeC_2B_4 clusters in these complexes are closely similar, their hydrocarbon regions are markedly different. This suggests that **2** forms via linkage or cocondensation involving the indene ligands on two **1** molecules,[10] but a crystallographic analysis would be required to confirm such a structure.

Compound **1** was readily decapitated (its apex BH unit removed[4a]) by treatment with tetramethylethylenediamine (TMEDA), affording the lemon-yellow species (η^6-C_9H_8)Fe($Et_2C_2B_3H_5$) (**3**) in 75% isolated yield. Given the accessibility of this complex, it should be a useful addition to the family of "building-block" reagents for constructing multidecker sandwiches;[4] however, this aspect of the chemistry of **3** was not pursued in the present study.

Table V. Bond Distances and Selected Bond Angles for **1**

		Bond Distances, Å			
Fe–C2	2.050 (3)	C2–B6	1.552 (5)	C3M–C3E	1.502 (6)
Fe–C3	2.058 (3)	C2–B7	1.765 (6)	C4–C5	1.397 (8)
Fe–B4	2.116 (4)	C2–C2M	1.521 (5)	C4–C12	1.385 (8)
Fe–B5	2.139 (4)	C3–B4	1.552 (5)	C5–C6	1.403 (7)
Fe–B6	2.117 (4)	C3–B7	1.747 (5)	C6–C7	1.488 (7)
Fe–C4	2.046 (4)	C3–C3M	1.515 (4)	C6–C10	1.393 (5)
Fe–C5	2.091 (4)	B4–B5	1.667 (6)	C7–C8	1.383 (8)
Fe–C6	2.119 (3)	B4–B7	1.771 (7)	C8–C9	1.375 (9)
Fe–C10	2.104 (3)	B5–B6	1.649 (7)	C9–C10	1.493 (6)
Fe–C11	2.082 (4)	B5–B7	1.726 (6)	C10–C11	1.393 (5)
Fe–C12	2.048 (4)	B6–B7	1.770 (7)	C11–C12	1.385 (7)
C2–C3	1.467 (4)	C2M–C2E	1.502 (6)		
		Bond Angles, deg			
B6–C2–C3	111.9 (3)			B4–B7–C3	52.3 (2)
B7–C2–C3	64.7 (2)			B5–B7–C2	93.6 (2)
B7–C2–B6	64.1 (2)			B5–B7–C3	94.2 (2)
C2M–C2–C3	119.9 (3)			B5–B7–B4	56.9 (2)
C2M–C2–B6	127.8 (3)			B6–B7–C2	52.1 (2)
C2M–C2–B7	134.5 (3)			B6–B7–C3	90.7 (2)
B4–C3–C2	112.6 (2)			B6–B7–B4	96.5 (3)
B7–C3–C2	65.9 (2)			B6–B7–B5	56.3 (2)
B7–C3–B4	64.6 (2)			C2E–C2M–C2	114.2 (4)
C3M–C3–C2	122.9 (3)			C3E–C3M–C3	112.3 (3)
C3M–C3–B4	124.0 (3)			C12–C4–C5	120.3 (5)
C3M–C3–B7	132.7 (2)			C6–C5–C4	118.9 (5)
B5–B4–C3	104.5 (3)			C7–C6–C5	132.5 (5)
B7–B4–C3	63.0 (2)			C10–C6–C5	119.9 (4)
B7–B4–B5	60.2 (2)			C10–C6–C7	107.5 (5)
B6–B5–B4	105.7 (3)			C8–C7–C6	106.0 (5)
B7–B5–B4	62.9 (2)			C9–C8–C7	112.8 (5)
B7–B5–B6	63.2 (2)			C10–C9–C8	105.9 (5)
B5–B6–C2	105.3 (3)			C9–C10–C6	107.7 (4)
B7–B6–C2	63.8 (2)			C11–C10–C6	121.0 (4)
B7–B6–B5	60.5 (2)			C11–C10–C9	131.2 (4)
C3–B7–C2	49.4 (1)			C12–C11–C10	118.7 (4)
B4–B7–C2	90.5 (2)			C11–C12–C4	121.3 (4)

Deprotonation and Haptotropic Rearrangement of 1. In order to make the C_5 ring in **1** aromatic and thus presumably susceptible to π-complexation to metal ions, the neutral orange compound was deprotonated by treatment with butyllithium in THF solution. The reaction conditions, particularly temperature, are crucial in this procedure. When conducted at −78 °C, the violet anion **1**$^-$ was formed as expected; addition of dry HCl gas to this species *without warming* regenerated **1** quantitatively. However, when the solution of **1**$^-$ was warmed to 0 °C, rapid conversion to the magenta anion (η^5-C_9H_7)Fe($Et_2C_2B_4H_4$)$^-$ (**4**$^-$) was observed. Protonation of this ion with HCl·Et_2O gave the neutral magenta complex (η^5-C_9H_7)FeH($Et_2C_2B_4H_4$) (**5**), whose structure is clearly apparent from its proton NMR spectrum, which shows that the C_6 ring is uncomplexed while the C_5 ring displays an upfield shift indicating coordination to iron. Additionally, the high-field resonance at δ −11.15 is diagnostic of an Fe–H hydride group. The protonation of **4**$^-$ is reversible, as demonstrated by the conversion of **5** back to **4**$^-$ on treatment with NaH (Scheme I).

Exposure of the diamagnetic iron(II) species **5** and **4**$^-$ to atmospheric oxygen followed by chromatography on silica produced the paramagnetic complex (η^5-C_9H_7)Fe($Et_2C_2B_4H_4$) (**4**) containing formal iron(III), as a dark gray/violet, slightly air sensitive crystalline solid, obtained in 90% isolated yield; reduction of this species with potassium metal in THF solution regenerated the anion **4**$^-$. The 17-electron complex **4** was examined via ESR spectroscopy conducted in toluene solution or toluene glass between 25 and −160 °C (Figure 2). At −160 °C $g_\parallel$ and $g_\perp$ were measured as 2.535 and 2.008, respectively, consistent with the presence of one unpaired electron in the vicinity of the iron atom and supporting the designation of a formal metal oxidation state of +3. These data can be compared to the ESR spectra of the diborolyl–carboranyl "hybrid" complex (η^5-$Et_2C_2B_4H_4$)Fe^{III}-($Et_2MeC_3B_2Et_2$)Co^{III}Cp measured under the same conditions[5] ($g_\parallel$ = 2.583 and $g_\perp$ = 2.000), as well as that of (C_5Me_5)Fe^{III}-

(9) (a) Pipal, J. R.; Grimes, R. N. *Inorg. Chem.* **1979**, *18*, 263. (b) Maynard, R. B.; Swisher, R. G.; Grimes, R. N. *Organometallics* **1983**, *2*, 500. (c) Micciche, R. P.; Sneddon, L. G. *Organometallics* **1983**, *2*, 674. (d) Boyter, H. A., Jr.; Swisher, R. G.; Sinn, E.; Grimes, R. N. *Inorg. Chem.* **1985**, *24*, 3810.

(10) Chemical and electrochemical dimerization of cyclopentadienyliron(I) benzene complexes has been observed; see: Astruc, D. *Tetrahedron* **1987**, *39*, 4027, and references therein.

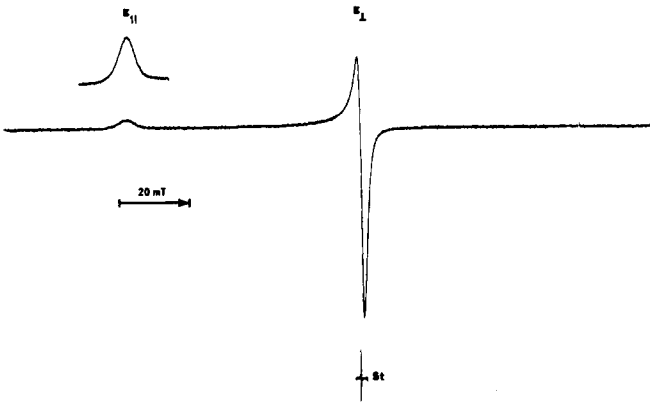

Figure 2. X-band ESR spectrum of **4** at −160 °C in toluene glass (standard, Li(TCNQ); $g = 2.0025$).

$(Et_2C_2B_4H_4)$[11] ($g_\parallel = 2.689$, $g_\perp = 1.979$). The similarity in these spectra supports the presumption of comparable electronic structures in this family of Fe(III)–carborane species.

Transition-metal migration between the η^6-C_6 and η^5-C_5 rings on an indenyl ligand has been observed only rarely[12] (although more frequently in metal–fluorene systems[13]). The complexes $(\eta^6\text{-}C_9H_8)M(\eta^5\text{-}C_5Me_5)^{2+}$ (M = Ir, Rh) were found to undergo spontaneous deprotonation and rearrangement to the $(\eta^5\text{-}C_9H_7)M(\eta^5\text{-}C_5Me_5)^+$ ions; protonation of the latter species in strong acids (the iridium complex required CF_3SO_3H) reversed the process, regenerating the η^6 dications.[12a] In a similar reaction, (η^5-indenyl)methylchromium tricarbonyl was thermally converted to the η^6-indenyl isomer in which the σ-CH_3 group has moved from the metal to the C_5 ring.[12b] To our knowledge, prior to the work reported here the only example of a haptotropic rearrangement in an iron–indenyl species was the conversion of bis(η^5-indenyl)iron to the (η^5-indenyl)(η^6-indene)iron(II) cation via protonation of the former complex[14a] or treatment of it with $BF_3{\cdot}Et_2O$.[14b] In the present case, the ability of the $Et_2C_2B_4H_4^{2-}$ ligand to stabilize both Fe(II) and Fe(III) via strong covalent bonding[4] is undoubtedly a factor in minimizing decomposition or side reactions of the indenyl complexes, thereby allowing both η^5- and η^6-complexes to exist at room temperature in solution.

Cluster Expansion of 1 and Related Complexes via Metal Insertion. As explained in the Introduction, part of our motivation for preparing indenyl–metal–carboranyl complexes was to convert these species to multilevel sandwich complexes by coordination of a second metal–ligand unit to the uncomplexed ring in compounds such as **1**. A trilevel (η^6:η^5-indenyl)-bridged compound of this type, $(CO)_3Cr(C_9H_7)Rh(C_8H_{12})$, was reported recently.[15] Accordingly, the anion **4**$^-$ was treated with $NiBr_2$ and $C_5Me_5^-$ in THF solution at −78 °C with gradual warming to room temperature, which produced a red solution from which red $(\eta^5\text{-}C_9H_7)Fe(Et_2C_2B_4H_4)Ni(C_5Me_5)$ (**6**) was isolated via plate chromatography in 35% yield (Scheme II). The first cluster expansion of **1** was observed when **4**$^-$, $NiBr_2$, and the diborolylcobalt anion[16] $CpCo(Et_2MeC_3B_2Et_2)^-$ were reacted to give red $(\eta^5\text{-}C_9H_7)Fe(Et_2C_2B_4H_4)Ni(Et_2MeC_3B_2Et_2)CoCp$ (**7**) in 30% isolated yield, as shown in Scheme II. It is apparent from their ^{11}B and ^1H NMR spectra that **6** and **7** have similar cage geometries, and that neither species has the anticipated indenyl-bridged staggered triple-decker structure. The boron spectra are radically different from those of the precursors **1** and **4**$^-$, both **6** and **7** having resonances at extremely low field (δ 117, 119); morever, in each spectrum the proton signals of the indenyl ligand show that only the C_5 ring, and not the C_6 ring, is complexed to a metal center.

Scheme II

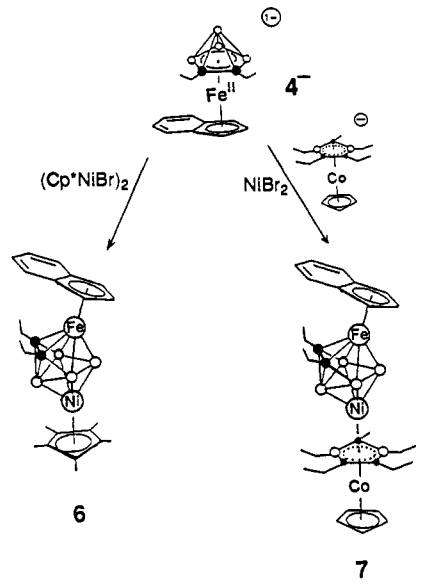

Table VI. Bond Distances and Selected Bond Angles for **6**

Bond Distances, Å					
Ni–Fe	3.373 (1)	B5–B6	1.828 (5)	C13–C18	1.518 (6)
Ni–B5	1.942 (4)	B5–H1	1.148 (30)	C14–C15	1.401 (5)
Ni–B1	1.939 (4)	B1–B6	1.890 (6)	C14–C19	1.519 (5)
Ni–B4	2.099 (4)	B1–C2	1.669 (5)	C15–C20	1.513 (6)
Ni–B6	2.112 (4)	B1–C3	1.685 (5)	C21–C22	1.418 (5)
Ni–C11	2.105 (3)	B1–H2	1.098 (35)	C21–C25	1.409 (5)
Ni–C12	2.086 (3)	B4–C3	1.583 (5)	C21–C26	1.428 (7)
Ni–C13	2.095 (3)	B4–H3	1.132 (30)	C22–C23	1.398 (6)
Ni–C14	2.109 (3)	B6–C2	1.594 (5)	C22–C29	1.426 (6)
Ni–C15	2.098 (3)	B6–H4	0.999 (32)	C23–C24	1.401 (6)
Fe–B5	1.913 (4)	C2–C3	1.457 (5)	C23–H15	0.943 (39)
Fe–B4	2.161 (4)	C2–C2M	1.519 (4)	C24–C25	1.392 (7)
Fe–B6	2.169 (4)	C3–C3M	1.526 (5)	C24–H16	0.826 (43)
Fe–C2	1.986 (3)	C2M–C2E	1.456 (6)	C25–H17	0.932 (42)
Fe–C3	1.992 (3)	C3M–C3E	1.445 (7)	C26–C27	1.342 (12)
Fe–C21	2.183 (3)	C11–C12	1.416 (6)	C26–H18	0.759 (48)
Fe–C22	2.187 (3)	C11–C15	1.430 (6)	C27–C28	1.345 (13)
Fe–C23	2.068 (4)	C11–C16	1.496 (6)	C27–H19	1.028 (87)
Fe–C24	2.039 (4)	C12–C13	1.401 (6)	C28–C29	1.329 (13)
Fe–C25	2.069 (4)	C12–C17	1.502 (6)	C28–H20	0.885 (88)
B5–B4	1.819 (6)	C13–C14	1.387 (5)	C29–H21	0.837 (52)

Bond Angles, deg			
Fe–B4–Ni	104.7 (1)	C19–C14–C15	126.1 (3)
Fe–B5–Ni	122.1 (2)	C14–C15–C11	107.7 (3)
B6–B5–B4	86.4 (2)	C20–C15–C11	127.1 (4)
Fe–B6–Ni	104.0 (1)	C20–C15–C14	125.1 (4)
B1–C3–Fe	104.2 (2)	C25–C21–C22	108.0 (3)
C2E–C2M–C2	115.0 (4)	C26–C21–C22	118.5 (5)
C3E–C3M–C3	115.8 (4)	C26–C21–C25	133.5 (5)
C15–C11–C12	106.9 (3)	C23–C22–C21	107.7 (3)
C16–C11–C12	126.5 (5)	C29–C22–C21	118.7 (5)
C16–C11–C15	126.6 (5)	C29–C22–C23	133.6 (5)
C13–C12–C11	108.0 (3)	C24–C23–C22	107.6 (4)
C17–C12–C11	125.8 (5)	C25–C24–C23	109.4 (4)
C17–C12–C13	126.1 (4)	C24–C25–C21	107.1 (4)
C14–C13–C12	108.8 (3)	C27–C26–C21	118.3 (8)
C18–C13–C12	124.8 (4)	C28–C27–C26	123.2 (8)
C18–C13–C14	126.3 (4)	C29–C28–C27	121.9 (7)
C15–C4–C13	108.6 (3)	C28–C29–C22	119.3 (7)
C19–C14–C13	125.3 (3)		

(11) Chase, K. J.; Stephan, M.; Grimes, R. N., unpublished. A report on the electrochemistry and other properties of a series of arene–ferracarboranes including **8** and related species will be presented separately.

(12) Experimental studies: (a) White, C.; Thompson, S. J.; Maitlis, P. M. *J. Chem. Soc., Dalton Trans.* **1977**, 1654. (b) Nesmeyanov, A. N.; Ustynyuk, N. A.; Makarova, L. G.; Andre, S.; Ustynyuk, Yu. A.; Novikova, L. N.; Luzikov, Yu. N. *J. Organomet. Chem.* **1978**, *154*, 45. Theoretical treatment: (c) Albright, T. A.; Hofmann, P.; Hoffmann, R.; Lillya, C. P.; Dobosh, P. A. *J. Am. Chem. Soc.* **1983**, *105*, 3396.

(13) An extensive list of references is cited in ref 12c.

(14) (a) Treichel, P. M.; Johnson, J. M. *J. Organomet. Chem.* **1975**, *88*, 207. (b) Lee, C. C.; Sutherland, R. G.; Thomson, B. J. *J. Chem. Soc., Chem. Commun.* **1971**, 171.

(15) Ceccon, A.; Gambaro, A.; Santi, S.; Valle, G.; Venzo, A. *J. Chem. Soc., Chem. Commun.* **1989**, 51.

(16) (a) Siebert, W.; Edwin, J.; Pritzkow, H. *Angew. Chem., Int. Ed. Engl.* **1982**, *21*, 148. (b) Edwin, J.; Boehm, M. C.; Chester, N.; Hoffman, D.; Hoffmann, R.; Pritzkow, H.; Siebert, W.; Stumpf, K.; Wadepohl, H. *Organometallics* **1983**, *2*, 1666.

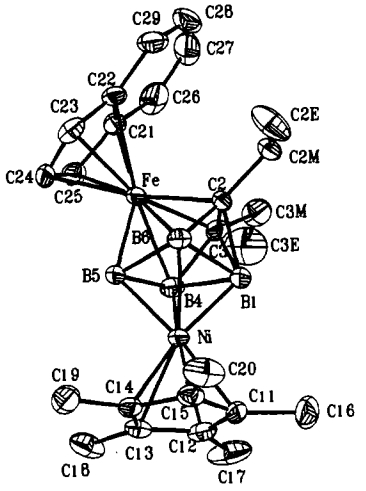

Figure 3. Molecular structure of **6**, with hydrogen atoms omitted.

Hence, it appeared that the nickel atom in these complexes resided in the polyhedral cluster rather than on the indenyl group. This has been confirmed by an X-ray diffraction study of **6**, which revealed the geometry shown in Figure 3. Data collection parameters, bond distances, and selected bond angles are listed in Tables IV and VI. The molecule incorporates an eight-vertex $FeNiC_2B_4$ dodecahedral cluster in which the nickel, cage carbon atoms, and one boron atom occupy 4-coordinate vertices while iron and the remaining borons reside in 5-coordinate vertices. Based on contributions of three skeletal electrons each from the Ni(ligand) and C–Et units, two from each BH, and one from the Fe(η^5-indenyl) group, the total of 18 conforms to the polyhedral skeletal electron counting theory[17] (Wade's rules) prediction of a closo eight-vertex polyhedron. It is notable that the iron is coordinated to the five-membered indenyl ring; this is consistent with the structure of the precursor 4^- ion described above, which was shown spectroscopically to have η^5-iron–indenyl coordination.

The bond distances and angles in **6** are within normal ranges and the cage geometry is that of a regular eight-vertex dodecahedron, save for the expected distortions arising from the different covalent radii of iron/nickel, carbon, and boron. There are no previous examples of crystallographically defined $M_2C_2B_4$ or $MM'C_2B_4$ single-cage species, although several wedged-type complexes having eight-vertex (monocapped seven-vertex) assemblies have been characterized.[18] The one earlier structure that can usefully be compared to **6** is that of $[(C_5Me_5)Co(Me_2C_2B_4H_3]_2CoH$, which consists of two closo eight-vertex $Co_2C_2B_4$ polyhedra that share a common cobalt vertex, and are also linked by a direct intercage B–B bond.[19] In that species, the arrangement of metal, carbon, and boron atoms in each cage corresponds exactly to that observed in **6**.

While no direct information on the mechanism of formation of **6** and **7** is available, it is apparent that these structures can be generated from 4^- by breaking the B5–B7 bond and inserting Cp*Ni or $CpCo(Et_2MeC_3B_2Et_2)Ni$ into the resulting hole. However, the curious question is *why* this happens. Indeed, we know of no clear precedent for conversion of a seven-vertex monometallacarborane to an eight-vertex dimetallacarborane cluster via metal addition. In general, metal insertion into closo boron clusters (polyhedral expansion[3,20]) is usually accomplished by reductive cage opening followed by insertion of a metal ion (e.g.,[21] $C_2B_{10}H_{12} + 2e^- \rightarrow C_2B_{10}H_{12}^{2-} \xrightarrow{CpCo^{2+}} CpCoC_2B_{10}H_{12}$), or via thermal reaction of a neutral closo species with a neutral metal reagent (e.g.,[22] $C_2B_5H_7 + CpCo(CO)_2 \rightarrow CpCoC_2B_5H_7 + 2CO$). The formation of **6** and **7** from 4^- does not fit neatly into either category and in this sense represents a new mode of cage expansion. A reasonable hypothesis is that that there is a net transfer of electron density from the indenyl ligand to the carborane ligand in 4^-, leading to some degree of cage opening or weakening of the B5–B7 bond and thus making the cage susceptible to metal insertion on treatment with the nickel reagents. A crystal structure of 4^- would clearly be of interest.

Scheme III

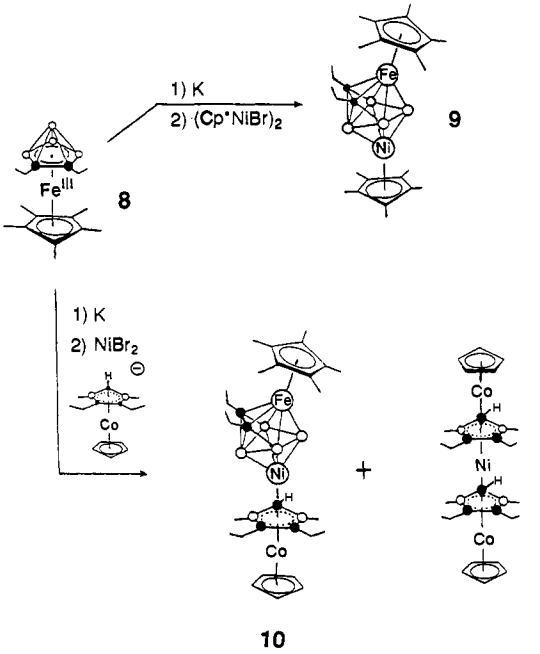

In order to explore further the scope of nickel insertions into FeC_2B_4 clusters, the known compound[11] $Cp^*Fe(Et_2C_2B_4H_4)$ (**8**), an analogue of **4**, was exposed to a potassium mirror and treated with LiCp* and $NiBr_2$, which produced the species $Cp^*Fe(Et_2C_2B_4H_4)NiCp^*$ (**9**) in 27% isolated yield (Scheme III). This reaction, in contrast to the formation of **6** and **7**, employs reductive cage opening with subsequent metal insertion and thus follows the pattern of earlier polyhedral expansions referred to above. The main point of interest here is whether the $FeNiC_2B_4$ cluster geometry of **9** is the same as that determined for **6** and **7**. That this is indeed the case is evident from the ^{11}B NMR chemical shifts, which (aside from the diborolyl resonance in **7**) are nearly identical for the three compounds. In an analogous reaction, **8** was treated with potassium, $NiBr_2$, and the $CpCo(Et_2HC_3B_2Me_2)^-$ anion (a diborole–cobalt complex different from that used in the preparation of **7**), forming in low yield an air-sensitive product, which was characterized as $Cp^*Fe(Et_2C_2B_4H_4)Ni(Et_2HC_3B_2Me_2)CoCp$ (**10**). The close similarity of the ^{11}B NMR spectrum to that of **7** strongly indicates that the two species have analogous $FeNiC_2B_4$ cage structures, as shown in Scheme III.

Electrochemistry. The compounds **1**, **3**, **4**, **5**, and **7** were investigated via cyclic voltammetry in 0.1 M Bu_4NPF_6/CH_2Cl_2 and Bu_4NPF_6/dimethoxyethane (DME) solutions at glassy carbon working electrodes. The 1-electron nature of the observed reversible signals was established from the observed peak currents of the waves in comparison to a 1-electron standard ($Cp_2Fe^{+/0}$). In addition, the differences between cathodic and anodic peak potentials (ΔE_p) of a redox couple were measured and compared to the behavior of Cp_2Fe under the same conditions. Separations of 60–80 mV were observed for reversible waves in CH_2Cl_2 at scan rates between 0.05 and 0.5 V/s, and slightly higher ΔE_p values were obtained in DME. The voltage ranges investigated were

(17) (a) Wade, K. *Adv. Inorg. Chem. Radiochem.* **1976**, *18*, 1. (b) Mingos, D. M. P. *Acc. Chem. Res.* **1984**, *17*, 311.
(18) (a) $CpCoFe(Me_2C_2B_4H_4)_2$: Maxwell, W. M.; Sinn, E.; Grimes, R. N. *J. Am. Chem. Soc.* **1976**, *98*, 3490. (b) $(Et_3P)_2CoFe(Me_2C_2B_4H_4)_2$ and $(Et_3P)_2PtFe(Me_2C_2B_4H_4)_2$: Barker, G. K.; Garcia, M. P.; Green, M.; Stone, F. G. A.; Welch, A. J. *J. Chem. Soc., Dalton Trans.* **1982**, 1679.
(19) Finster, D. C.; Sinn, E.; Grimes, R. N. *J. Am. Chem. Soc.* **1981**, *103*, 1399.
(20) Dunks, G. B.; Hawthorne, M. F. *J. Am. Chem. Soc.* **1970**, *92*, 7213.
(21) Dustin, D. F.; Dunks, G. B.; Hawthorne, M. F. *J. Am. Chem. Soc.* **1973**, *95*, 1109.
(22) Miller, V. R.; Sneddon, L. G.; Beer, D. C.; Grimes, R. N. *J. Am. Chem. Soc.* **1974**, *96*, 3090.

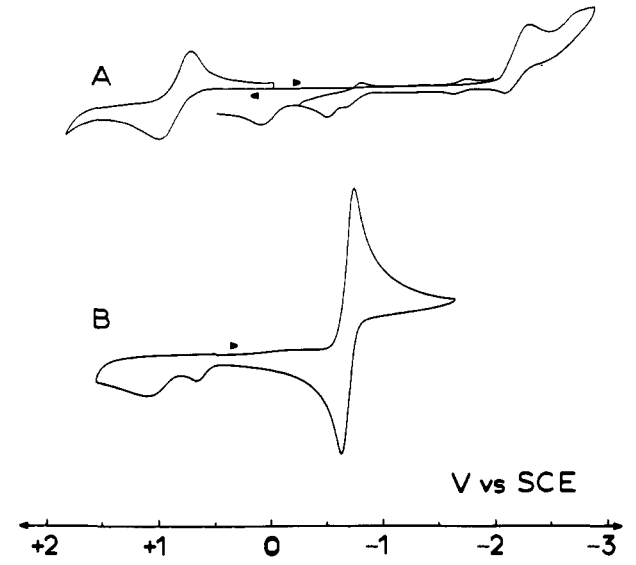

Figure 4. Cyclic voltammograms for **1** and **4** at GC electrodes vs SCE at 20 °C. (A) **1** in 0.1 M Bu_4NPF_6/DME, scan rate 0.5 V/s; $1^{+/0}$ $E°$ = +0.92 V. (B) **4** in 0.1 M Bu_4NPF_6/CH_2Cl_2, scan rate 0.1 V/s; $E°$ = −0.64 V.

Scheme IV

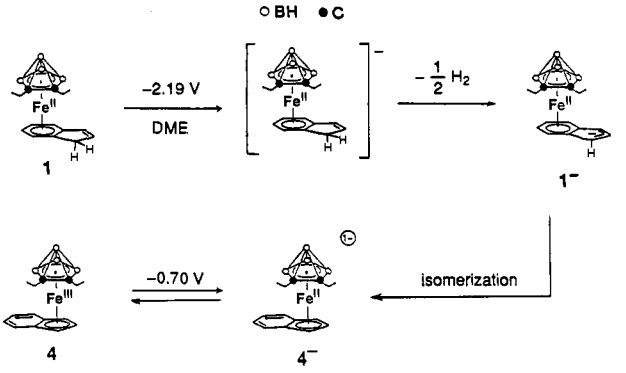

+2.60 to −2.20 V in CH_2Cl_2 and +2.00 to −3.10 V in DME at a ground current sensitivity of 5 μA/cm.

Cyclic voltammetry on **1** exhibited a reversible 1-electron oxidation wave at scan rates between 0.05 and 20 V/s. The value of $E°$ +0.92 V vs SCE was measured as solvent independent in CH_2Cl_2 and DME. At a scan rate of 0.2 V/s the ratio of peak currents (i_c/i_a) was 0.98 and ΔE_p was 67 mV. In CH_2Cl_2 a second, irreversible, oxidation wave was observed at +1.99 V (E_p^{ox}, v = 0.1 V/s). Owing to the extended electrochemical window of DME, a 1-electron reduction wave was detected. This signal is irreversible (E_p^{red} = −2.19 V; v = 0.1 V/s) at room temperature and scan rates up to 2 V/s. As shown in Figure 4A, the reduction of **1** leads to the formation of several new species, which give rise to three reversible waves ($E°$ = −1.68, −0.70, and −0.53 V), which were clearly visible on the oscilloscope at a 5 V/s scan rate. The signal at $E°$ = −0.70 V is at the same potential as the couple $\mathbf{4}^{0/-}$ (see below). This is consistent with the chemistry described above (Scheme I), but the appearance of additional waves arising from unspecified products suggests a complex reaction pattern. One possible pathway leading to the formation of $\mathbf{4}^-$ involves an ECCE-type mechanism (E, electron transfer; C, chemical reaction) as depicted in Scheme IV.

The decapped complex **3** exhibited an irreversible oxidation wave at +0.98 V (E_p^{ox}, v = 0.2 V/s), which is close to the peak potential for the oxidation of the couple $\mathbf{1}^{+/0}$. As observed earlier on other species containing the open-faced $Et_2C_2B_3H_5^{2-}$ ligand, adsorption processes occurring after oxidation rapidly alter the surface of the working electrode.[6,23] In DME, **3** reduces irreversibly at −2.65 V (E_p^{red}, v = 0.2 V/s), with formation of a following product (E_p^{ox} = −0.64 V, v = 0.2 V/s).

(23) Hu, D.; Zenneck, U., unpublished results.

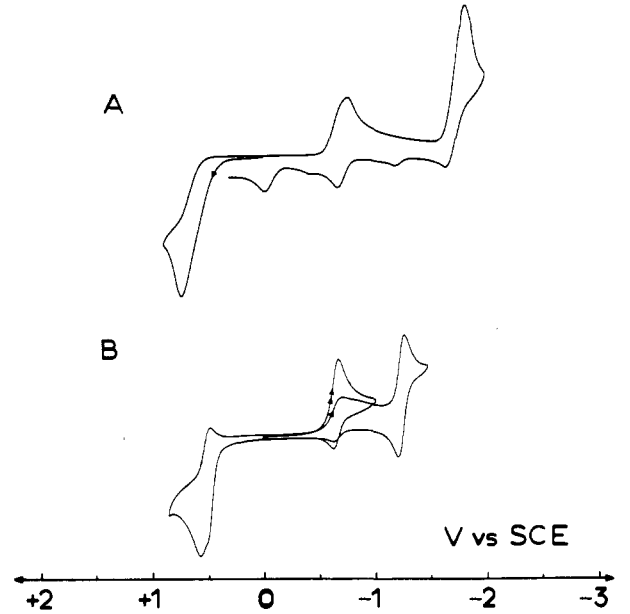

Figure 5. Cyclic voltammograms at GC electrodes vs SCE at 20 °C in 0.1 M Bu_4NPF_6/CH_2Cl_2, scan rate 0.1 V/s. (A) **5**; (B) **7**.

These results provide further strong evidence of the ability of the $Et_2C_2B_4H_4^{2-}$ ligand to stabilize the Fe(III) oxidation state in iron–arene complexes, as observed earlier in (η^6-C_5H_6)Fe-($Et_2C_2B_4H_4$) ($E°$ = +1.01 V vs SCE in CH_2Cl_2) and related species.[24] Relative to the benzene complex, the η^6-indene ligand shifts the Fe(II)/Fe(III) wave in the negative direction by ~0.1 V, suggesting that the adjoining C_5 ring slightly stabilizes the monocation $\mathbf{1}^+$. In contrast, the decapped complex **3** (whose $Et_2C_2B_3H_5^{2-}$ ligand is isoelectronic and isolobal with $Et_2C_2B_4H_4^{2-}$) does not form a stable cation. Similar observations have been made in cyclic voltammetric studies of CoCo[6] and FeCo[5] triple-decker complexes containing the $Et_2C_2B_3H_5^{2-}$ unit. These findings are paralleled by our inability to prepare an iron(III) complex of this open carborane ligand. Clearly, the elimination of the apical BH unit in $Et_2C_2B_4H_4^{2-}$ complexes (as, for example, in the conversion of **1** to **3**) substantially lowers the ability of the ligand to stabilize higher oxidation states. A qualitative rationale would be that the planar C_2B_3 *end-capping* ligand is less effective as an electron sink or reservoir than is the pyramidal C_2B_4 unit, which forms a closo seven-vertex cluster on coordination to a metal. This would not, of course, apply to planar $R_2C_2B_3H_3^{4-}$ bridging ligands in multidecker complexes, since in this case both faces are coordinated to metals creating a closo cluster; indeed, such species readily form stable cations.[7,25]

The paramagnetic Fe(III) complex **4** undergoes a diffusion-controlled 1-electron reduction in both solvents, giving $E°$ values of −0.64 V in CH_2Cl_2 (see Figure 4B) and −0.70 V in DME. In CH_2Cl_2, ΔE_p was measured as 65 mV at 0.1 V/s scan rate, exhibiting the same behavior as the $Cp_2Fe^{+/0}$ wave at scan rates between 0.02 and 1 V/s; a peak current ratio of 0.99 was observed in all cases. Two irreversible oxidation states were found at +0.65 and +1.60 V (E_p^{ox}, v = 0.2 V/s). Strong support for the assignment of a formal Fe(III) oxidation state, and a reduction process corresponding to an Fe(III)/Fe(II) couple, is given by the ESR spectrum of **4**, which was described above.

The electrochemical behavior of the η^5-indenyliron hydride complex **5**, shown in Figure 5A, proved somewhat easier to interpret. Cyclic voltammograms of freshly prepared **5** in CH_2Cl_2

(24) Merkert, J. M.; Geiger, W. E.; Davis, J. H., Jr.; Attwood, M. D.; Grimes, R. N. *Organometallics* **1989**, *8*, 1580.

(25) (a) Brennan, D. E.; Geiger, W. E., Jr. *J. Am. Chem. Soc.* **1979**, *101*, 3399. (b) Merkert, J.; Davis, J. H., Jr.; Grimes, R. N.; Geiger, W. *Abstracts of Papers*, American Chemical Society National Meeting, Boston, MA, April 1990; American Chemical Society: Washington, DC, 1990; INOR 92.

Scheme V

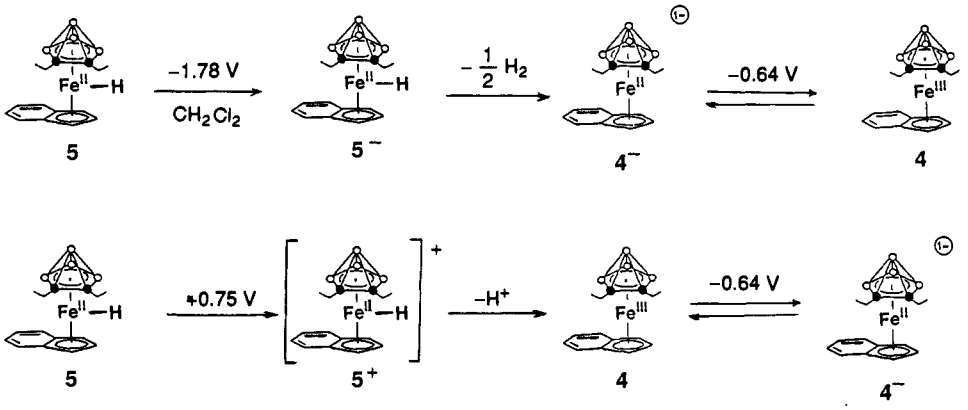

gave irreversible signals at −1.78 V (E_p^{red}, v = 0.1 V/s), and at +0.75 V (E_p^{ox}, v = 0.1 V/s). The oxidation was followed by a reversible signal at $E°$ = −0.64 V, whereas the reduction gave, in addition to a reversible signal, three irreversible waves at −1.18, −0.43, and −0.04 V (E_p^{ox}, v = 0.1 V/s). The values obtained in DME were shifted slightly to the negative, but clearly there is no significant solvent dependence; thus, $E°$ of the reversible wave was −0.70 V. For the reduction signal at −1.78 V, a reoxidation wave became significant at scan rates higher than 0.2 V/s with a peak current ratio of 0.3 at a scan rate of 0.5 V/s at room temperature. This indicates that a short-lived species, 5^-, is generated in the same scale of the experiment.

These data suggested that **5** could be electrochemically transformed into **4** via oxidation followed by reduction to 4^-. As noted above, **5** on exposure to air yields **4** quantitatively; this was manifested electrochemically by the disappearance of the waves of **5** as air was bubbled through the cell. Concurrent with this, the wave having $E°$ = −0.70 V, having a cyclic voltammogram identical with that of **4**, was seen. The irreversible reduction of **5** was more complex, generating byproducts that gave rise to three irreversible signals. However, an ECE-type mechanism can be postulated for both oxidation and reduction, as shown in Scheme V. Further investigations of this system employing ring–disk electrodes, preparative electrolysis, and comparison with the related species **8** are planned.

The cyclic voltammogram of **7** in CH_2Cl_2 (Figure 5B) indicated considerable decomposition to form **4** on oxidation; the peak current i_p^{red} sharply increased following irreversible oxidation at +0.62 V (E_p^{ox}, v = 0.1 V/s). A reduction wave with $E°$ = −1.25 V was observed in CH_2Cl_2, with a peak separation of 72 mV and i_a/i_c = 0.93.

Conclusions

The chemistry of the indene–iron–carborane sandwich **1**, as described in this study, provides a particularly illuminating example of the utilization of small carborane ligands in stabilizing unusual transition-metal organometallic species. This has permitted not only the generation, but also the isolation and full characterization, of a number of complexes of varying metal oxidation state and metal–hydrocarbon hapticity, to a degree that is rarely possible in systems employing metals and hydrocarbon ligands alone. For example, the power of the $R_2C_2B_4H_4^{2-}$ ligands to stabilize Fe(III)–arene species (otherwise virtually unknown[26]), and to allow migration of iron on an indenyl ligand (also rare), leaves no doubt that these ligands are tools of extraordinary power for organometallic synthesis, their "boron chemistry" origin notwithstanding. The observed polyhedral expansion of the FeC_2B_4 cage by nickel insertion adds an unexpected further dimension to this chemistry, which reminds us that the carborane ligands have not only a stabilizing role as described, but are also capable of manifesting their cluster nature under appropriate conditions. We anticipate further exploration of both kinds of phenomena in future studies, as well as more detailed investigation of the electronic structures and properties of the eight-vertex clusters.

Experimental Section

Except where otherwise indicated, materials, instrumentation, and general procedures were identical with those described elsewhere.[6] Unless otherwise stated, operations were conducted in the vacuum line or under a nitrogen atmosphere. All new products gave unit-resolution mass spectra in good agreement with calculated spectra, supported by high-resolution mass measurements. In addition, the fragmentations exhibited in the unit-resolution spectra are consistent with the proposed structures, e.g., loss of ligand or M(ligand) units from the parent ions. ^{13}C NMR spectra were obtained at 75.5 MHz.

Synthesis of (η^6-C_9H_8)Fe($Et_2C_2B_4H_4$) (1). A 300-mg (1.0 mmol) sample of (η^6-C_8H_{10})Fe($Et_2C_2B_4H_4$)[27] was placed with 2.5 mL of indene in a thick-walled Pyrex tube and degassed by several freeze–thaw cycles, sealed under vacuum while frozen in liquid nitrogen, and heated to 180 °C for 1.5 h. During this time the solution gradually darkened. The tube was cooled and opened in air, and the excess indene was removed in vacuo over a 2-h period. The residue was dissolved in CH_2Cl_2 and passed through a silica column. Chromatography of the eluate on silica in 3:1 hexane/CH_2Cl_2 gave, as the main band (R_f 0.2), pure **1** as bright yellow-orange crystals (250 mg, 0.83 mmol, 83% yield), mp 95–96 °C, which are soluble in ether but dissolve only slightly in hexane. A minor band (R_f 0.05) was isolated in ca. 5% yield as orange crystals and characterized as a dimeric species, [(C_9H_7)Fe($Et_2C_2B_4H_4$)]$_2$ (**2**). Exact mass for **1**: calcd for $^{56}Fe^{12}C_{15}{}^{11}B_4{}^1H_{22}{}^+$, 302.1443, found 302.1444. Exact mass for **2**: calcd for $^{56}Fe_2{}^{12}C_{30}{}^{11}B_8{}^1H_{42}{}^+$, 602.2730, found 602.2712. ^{13}C NMR of **1** ($CDCl_3$ solution, δ referenced to $SiMe_4$ = 0): 138.5 (C=C), 130.2 (C=C), 105.0 (aryl), 101.3 (aryl), 90 (br, BC), 81.3 (aryl), 80.1 (aryl), 80.0 (aryl), 78.8 (aryl), 39.3 (indene CH_2), 23.8 (ethyl CH_2), 23.5 (ethyl CH_2), 15.0 (CH_3), 14.1 (CH_3).

Synthesis of (η^6-C_9H_8)Fe($Et_2C_2B_3H_5$) (3). A 70-mg (0.23 mmol) sample of **1** was dissolved in 2 mL of wet TMEDA and heated to 80 °C for 30 min, after which the TMEDA was removed by evaporation and the yellow residue dissolved in CH_2Cl_2. The solution was filtered through silica and chromatographed on silica in hexane, affording **3** as a viscous, air-stable lemon-colored oil, which dissolves readily in hexane (in contrast to **1**), yield 54 mg (0.18 mmol, 80%). Exact mass for **3**: calcd for $^{56}Fe^{12}C_{15}{}^{11}B_3{}^1H_{23}{}^+$, 292.1428, found 292.1417. ^{13}C NMR ($CDCl_3$ solution): δ 137.2 (C=C), 131.3 (C=C), 109 (br, BC), 106.2 (aryl), 103.2 (aryl), 85.4 (aryl), 83.6 (aryl), 82.7 (aryl), 81.5 (aryl), 39.5 (indene CH_2), 25.2 (ethyl CH_2), 24.9 (ethyl CH_2), 17.3 (CH_3), 17.2 (CH_3).

Conversion of 1 to (η^5-C_9H_7)Fe($Et_2C_2B_4H_4$)$^-$ (4^-) and (η^5-C_9H_7)FeH($Et_2C_2B_4H_4$) (5). A solution of 60 mg (0.20 mmol) of **1** in a minimal volume of THF was cooled to 0 °C and 1 equiv of *n*-butyllithium was added through a rubber septum, producing an immediate darkening of the yellow solution as the violet anion 4^- formed. After being stirred for 30 min at room temperature, the solution was cooled again to 0 °C and an excess of HCl·Et_2O was added via syringe, causing rapid lightening of the color. The solvent was removed and the residue was dissolved in hexane and chromatographed on a silica TLC plate under a nitrogen atmosphere in a glovebox. One major band, isolated as a magenta, air-sensitive solid, was **5**, yield 24 mg (40%). Complex **5** was also prepared from the paramagnetic species **4**. A 100-mg (0.33 mmol) sample

(26) The only other reported case of (arene)Fe^{III} stabilization, to our knowledge, is the reversible oxidation of the 1,3-diphosphete complex (η^6-MeC_6H_5)Fe^{II}($Bu_2C_2P_2$). See: Driess, M.; Hu, D.; Pritzkow, H.; Schäufele, H.; Zenneck, U.; Regitz, M.; Rösch, W. *J. Organomet. Chem.* **1987**, *334*, C35.

(27) Swisher, R. G.; Grimes, R. N. *Organomet. Synth.* **1986**, *3*, 104.

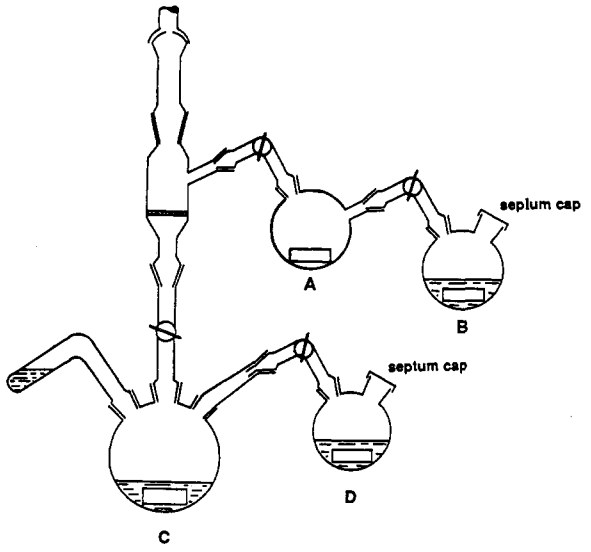

Figure 6. Apparatus for preparation of **9** (see text).

of the latter compound was dissolved in THF at −40 °C and warmed to room temperature, 15 mg (0.38 mmol) of potassium metal was added, and the mixture stirred for 2 h. $HCl{\cdot}Et_2O$ (0.5 mL, 0.33 mmol) was added and the workup was conducted as before, affording 54 mg (0.18 mmol, 54% yield) of magenta **5**. Exposure of this compound to oxygen resulted in complete conversion to the paramagnetic complex **4**. When the deprotonation of **1** was conducted in THF at −78 °C, addition of an excess of dry HCl gas to the anion solution regenerated **1** quantitatively. Exact mass for **5**: calcd for $^{56}Fe^{12}C_{15}{}^{11}B_4{}^1H_{22}{}^+$, 302.1443, found 302.1444. ^{13}C NMR of **5** ($CDCl_3$ solution): δ 127.2 (indenyl), 126.9 (indenyl), 93 (br, BC), 89.5 (indenyl), 70.7 (indenyl), 62.7 (indenyl), 23.3 (ethyl CH_2), 15.6 (CH_3).

Synthesis of $(\eta^5\text{-}C_9H_7)Fe(Et_2C_2B_4H_4)$ (4). A sample of 120 mg (0.40 mmol) of **1** was deprotonated in THF solution at 0 °C to give $\mathbf{4}^-$ as described above, and the solution was stirred for 30 min at 25 °C after which the solution was opened to the air and stirred for 1 h. Following solvent removal, plate chromatography in hexane gave dark gray/violet solid **4**, yield 110 mg (0.37 mmol, 92%). The compound is moderately air sensitive and is stored under nitrogen. Exact mass for **4**: calcd for $^{56}Fe^{12}C_{15}{}^{11}B_4{}^1H_{21}{}^+$, 301.1365, found 301.1369.

Synthesis of $(\eta^5\text{-}C_9H_7)Fe(Et_2C_2B_4H_4)NiCp^*$ (6). A solution of 54 mg of pentamethylcyclopentadiene (0.40 mmol) in THF was deprotonated via addition of 1 equiv of butyllithium and stirred for 1 h, and the solution was added slowly at 0 °C to a suspension of 87 mg (0.40 mmol) of $NiBr_2$ in THF, during which a color change to brown was noted. The combined suspension was stirred at 0 °C for 1 h. A solution of $Li^+\text{-}\mathbf{4}^-$ was prepared separately by deprotonation of 120 mg (0.40 mmol) of **1** with butyllithium at 0 °C as described above. The violet solution was stirred for 1 h. The solution of $(Cp^*NiBr)_x$ was frozen in liquid nitrogen and the $Li^+\text{-}\mathbf{4}^-$ solution was filtered into it in vacuo. The reaction mixture was placed in a −78 °C bath for 45 min, warmed to 0 °C and stirred overnight. The red solution was evaporated to dryness on the vacuum line and the residue taken into the glovebox and plated on silica, giving a single red band of **6**, yield 70 mg of red crystals, mp 172–174 °C (0.14 mmol, 35%). Exact mass for **6**: calcd for $^{60}Ni^{56}Fe^{12}C_{25}{}^{11}B_4{}^1H_{36}{}^+$, 496.1847, found 496.1848. ^{13}C NMR ($CDCl_3$ solution): δ 125.6 (indenyl), 124.9 (indenyl), 102.00, 91.0, 87.7 (br, BC), 72.5, 23.8 (ethyl CH_2), 15.2 (CH_3), 10.0 (CH_3).

Synthesis of $(\eta^5\text{-}C_9H_7)Fe(Et_2C_2B_4H_4)Ni(Et_2MeC_3B_2Et_2)CoCp$ (7). A 100-mg (0.32 mmol) sample of $CpCo(Et_2MeHC_3B_2Et_2)$[16] was deprotonated with 1 equiv of butyllithium in THF at −78 °C and the solution stirred for 10 min. A separate solution of $Li^+\text{-}\mathbf{4}^-$ (100 mg, 0.32 mmol) was prepared as described above. Both solutions were filtered in vacuo onto a frozen suspension of $NiBr_2$ (70 mg, 0.32 mmol) in DME at −196 °C. The mixture was placed in a −78 °C bath and stirred overnight, during which the solution turned red-brown. The solvent was removed on the vacuum line and the reddish residue was taken into the glovebox and plated on silica, giving one major red fraction (R_f 0.80) as well as some of the cobalt–diborole starting material (R_f 0.85). The major band was **7**, yield 65 mg (0.10 mmol, 30%). Exact mass for **7**: calcd for $^{60}Ni^{59}Co^{56}Fe^{12}C_{32}{}^{11}B_6{}^1H_{49}{}^+$, 674.2382, found 674.2404.

Synthesis of $Cp^*Fe(Et_2C_2B_4H_4)NiCp^*$ (9). The apparatus shown in Figure 6 was charged with 200 mg (0.62 mmol) of **8** in flask B, 200 mg (5.15 mmol) of surface-clean chunks of potassium metal in flask A, and 136 mg (0.62 mmol) of $NiBr_2$ in the sidearm of flask C. The entire apparatus was attached to the vacuum line and evacuated. The potassium metal was gently heated under vacuum to form a mirror on the surface of flask A. THF (50 mL each) was condensed into flasks B, C, and D, 89 mg (0.65 mmol) of pentamethylcyclopentadiene was added to flask D via syringe, and 0.38 mL of 1.7 M butyllithium was added to flask D. The suspension of $LiCp^*$ was stirred for 1.5 h, during which the suspension of $NiBr_2$ was stirred vigorously. The $LiCp^*$ was added dropwise to the $NiBr_2$ at room temperature, the color turning to brown and then nearly black. Stirring was continued for 2 h, during which the solution of **8** in THF was added in vacuo to flask A at room temperature. The solution was stirred for 1.5 h, during which it turned orange and parts of the potassium mirror disappeared. This solution was then filtered into the frozen solution of $(Cp^*NiBr)_x$ in flask C, which was placed in a −78 °C bath and stirred overnight while slowly warming to room temperature. The solvent was removed from the dark red solution in vacuo, and the residue was dissolved in CH_2Cl_2 in the glovebox and chromatographed on silica plates. Two bands were obtained, consisting of unreacted ferracarborane (**8**) and red, air-stable **9**, yield 87 mg (27% based on **8** consumed). Exact mass for **9**: calcd for $^{60}Ni^{56}Fe^{12}C_{26}{}^{11}B_4{}^1H_{44}{}^+$, 516.2473, found 516.2449.

Synthesis of $Cp^*Fe(Et_2C_2B_4H_4)Ni(Et_2HC_3B_2Me_2)CoCp$ (10). A procedure similar to that employed in the preparation of **9** was followed. A 118-mg sample (0.37 mmol) of **8** was reduced by exposure to a potassium mirror as described above. Separately, 100 mg (0.37 mmol) of $CpCo(Et_2H_2C_3B_2Me_2)$[28] (a lower homologue of the cobalt–diborolyl complex employed in the preparation of **7**) was deprotonated with butyllithium in THF at −50 °C. The two solutions were filtered in vacuo to a suspension of $NiBr_2$ in THF frozen in liquid nitrogen, the mixture was placed in a bath at −78 °C, and the green solution was stirred overnight. The residue was dissolved in CH_2Cl_2 and chromatographed on silica plates in the glovebox, affording three bands. The first (major) band was identified as the green tetradecker complex $[CpCo(Et_2HC_3B_2Me_2)]_2Ni$, which has been described previously.[28] The second band was brown **10**, yield 24 mg (15%), and the third band was unreacted cobalt–diborolyl starting material (36 mg). Compound **10** is air-sensitive, decomposing to give primarily **8**. Exact mass for **10**: calcd for $^{60}Ni^{59}Co^{56}Fe^{12}C_{30}{}^{11}B_6{}^1H_{51}{}^+$, 652.2538, found 652.2571.

X-ray Structure Determinations on 1 and 6. For both compounds, intensities were collected on a Siemens-Stoe 4-circle diffractometer, using the ω-scan technique, with data collection parameters as given in Table IV. The structures were solved by the heavy atom method and refined by least-squares calculations employing anisotropic thermal parameters for all non-hydrogen atoms. Reflections for which $I > 2\sigma(I)$ were considered observed (*hkl* −9,0,0 to 9,17,16 for **1**; −18,0,0 to 18,11,26 for **6**). Only these reflections were employed in the final refinement of structural parameters. Empirical absorption corrections (parameters in Table IV) were applied in both cases. For **1**, all hydrogens other than those on C2E were located and refined isotropically. The methyl hydrogens on C2E were refined as a rigid group (C–H distance = 0.95 Å) with a common isotropic temperature factor for hydrogen. For **6**, the four B–H hydrogen atoms and those on the indene ligand were refined isotropically, while the methyl hydrogens were refined as rigid groups. The CH_2 hydrogens were included in calculated positions with C–H = 0.95 Å. The refinements converged to the R and R_w values given in Table IV. Scattering factors were taken from Cromer and Mann.[29] All calculations were carried out using the programs SHELTX76 and SHELX86.[30]

Electrochemical Procedures. Purification of electrolytes and solvents, and all measurements, were conducted under argon. Tetrabutylammonium hexafluorophosphate (Fluka electrochemical grade) was dried at 110 °C for 20 h in vacuo before use. Dichloromethane (Merck p.a., Riedel-de Haen 99+%) was refluxed over calcium hydride and fractionated. DME (Aldrich 99+%) was passed through a column of activated basic alumina (ICN alumina B Super 1, activated at 280 °C for 2 days under vacuum), refluxed over CaH_2, and fractionated twice before use. The solvents were stored under argon in the dark in flasks equipped with Teflon stopcocks. Freshly prepared solutions of the electrolyte were stored in 100-mL Schlenk tubes of similar design. Preparation of the cell, electrodes, and the experimental procedures were as described elsewhere.[31]

Acknowledgment. This work was supported by the U.S. Army

(28) Edwin, J.; Bochmann, M.; Boehm, M. C.; Brennan, D. E.; Geiger, W. E., Jr.; Kruger, C.; Pebler, J.; Pritzkow, H.; Siebert, W.; Swiridoff, W.; Wadepohl, H.; Weiss, J.; Zenneck, U. *J. Am. Chem. Soc.* **1983**, *105*, 2582.
(29) Cromer, D. T.; Mann, J. B. *Acta Crystallogr.* **1968**, *A24*, 321.
(30) Sheldrick, G. M. SHELX76 program for crystal structure determination, Cambridge, 1976; SHELXS86, Göttingen, 1986.
(31) (a) Zwecker, J.; Kuhlmann, T.; Pritzkow, H.; Siebert, W.; Zenneck, U. *Organometallics* **1988**, *7*, 2316. (b) Stephan, M., Diplomarbeit, Universität Heidelberg, 1989.

Research Office (to R.N.G.), National Science Foundation Grant CHE 8721657 (to R.N.G.), the Deutsche Forschungsgemeinschaft SFB 247 (to W.S. and U.Z.), and NATO International Collaborative Research Grant 0196/85.

Supplementary Material Available: Tables of atom coordinates, thermal parameters, and mean planes (7 pages); calculated and observed structure factors (17 pages). Ordering information is given on any current masthead page.

Rediscovery of Photochromic Osazones: Photochromism and Molecular Structure of Mesoxaldehyde 1-Allyl-1-phenyl-2-phenylosazone[1]

Keiichiro Hatano,* Tadayuki Uno, Koji Kato, Tadahiro Takeda, Taku Chiba, and Setsuzo Tejima

Contribution from the Faculty of Pharmaceutical Sciences, Nagoya City University, Mizuho-ku, Nagoya 467, Japan. *Received April 16, 1990. Revised Manuscript Received December 3, 1990*

Abstract: A new photochromic family of osazones has been rediscovered. Mesoxaldehyde 1-allyl-1-phenyl-2-phenylosazone (IId) is photochromic both in solution and in the solid state. A pale yellow solution of IId changes to an orange solution when exposed to light. The exposed solution reverts to its original color with the addition of either acid or base. The decoloration is an acid–base-catalyzed reaction with clean first-order kinetics. The three-dimensional molecular structure of the unexposed crystal was determined by the X-ray crystallography. The presence of a planar chelate ring has been confirmed for the structure of the osazone. A hydrogen-transfer tautomerism in the chelate is a possible mechanism for the osazone photochromism.

The recent rapid growth in the study of erasable, optically read, and written memories demands the development and reassessment of what is known about photochromic substances. Photochromic substances were extensively reviewed by Brown in 1971.[3] Although some classic osazones are known to be photochromic in the solid state,[4] there has been no study carried out on photochromism of the osazone derivatives since one of the authors (ST) reported on their "phototropy" in 1952.[5] Mesoxaldehyde derivatives of osazones (II, Scheme I), prepared at that time, have been preserved for 40 years. The present paper reports our reinvestigation of the photochromism and the crystal structure of one of these compounds, mesoxaldehyde 1-allyl-1-phenyl-2-phenylosazone (IId).

Experimental Section

Materials and Methods. The series II was synthesized from glucosazones (I) by oxidation with 3 molar equiv of periodic acid as shown in Scheme I. Synthesis and chemical data for all of II have been reported,[5] and some of them, IIc, IId, and IIf, are photochromic in the solid state. We focus on IId in the present paper. The photochromic properties and the molecular structure of some other derivatives will be reported elsewhere.[6] The melting point (112 °C) of IId has been reconfirmed. Dichloromethane was distilled from CaH_2. All other reagents were obtained commercially and used without further purification.

A stock solution of IId in dichloromethane was prepared and stored in the dark. The sample solutions were prepared by using the stock solution and were adjusted from 20 to 100 μM in IId concentration in a 1-cm quartz cell. Irradiation was carried out with light from a 500-W xenon short arc Wacom lamp filtered by a Toshiba C-39A glass filter

Scheme I

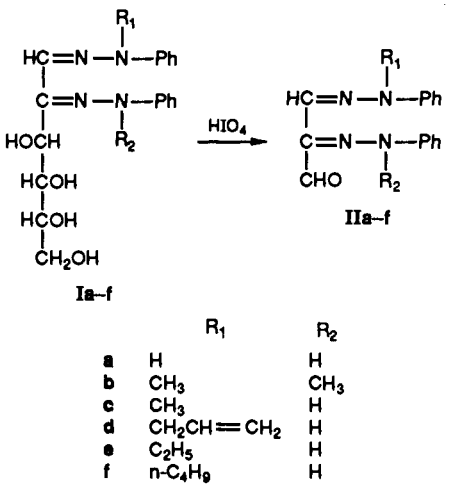

(transmission maximum 390 nm, 64%) on the sample solutions. The incident light intensity of 2×10^{16} quanta cm^{-2} s^{-1} was determined by potassium ferrioxalate actinometry. UV–vis spectra were recorded on a Shimadzu UV-2100 spectrometer.

X-ray Diffraction. Diffraction data were measured with graphite-monochromated Mo Kα radiation on an Enraf-Nonius CAD4 diffractometer. The θ–2θ scan technique was used with a variable scan rate. Crystal data are as follows: $C_{18}H_{18}N_4O$ fw = 306.4, monoclinic, a = 18.868 (4) Å, b = 5.350 (1) Å, c = 17.198 (2) Å, β = 108.54 (1)°, V = 1646.1 (77) Å^3, Z = 4, space group $P2_1/c$, ρ_{calcd} = 1.236 g/cm^3, 1177 observed data to 2θ = 50.0°, temperature = 20 ± 1 °C. The structure was solved and refined by using the SDP software package from Enraf-Nonius: R_1 = 0.094, R_2 = 0.087.

Results and Discussion

Photochromism of IId in Solution. When a pale yellow solution of IId (3.6×10^{-5} M) in dichloromethane was irradiated near its main absorption band (λ_{max} = 413 nm, ϵ = 20 100 M^{-1} cm^{-1}) at room temperature, the spectrum changed, and new absorption bands at longer wavelength (λ_{max} = 457 nm, ϵ = 19 000 M^{-1} cm^{-1}) appeared (Figure 1). The conversion to the colored form was completed within 2 min in dilute solution with clean isosbestic

(1) The nomenclature in this paper is in accord with ref. 2, while the correction of the chemical structure of ref 5 has been made, cf.: Tejima, S. *J. Pharm. Soc. Jpn.* **1957**, *77*, 673.

(2) (a) Mester, L.; Major, A. *J. Am. Chem. Soc.* **1957**, *79*, 3232. (b) Chapman, O. L.; King, R. W.; Welstead, W. J., Jr.; Murphy, T. J. *J. Am. Chem. Soc.* **1964**, *86*, 4968.

(3) Brown, G. H. In *Techniques of Chemistry, Vol. III, Photochromism*; Brown, G. H., Ed.; Wiley-Interscience: New York, 1971; p 1. (See, also, other chapters in this book.)

(4) References cited: Exelby, R.; Grinter, R. *Chem. Rev.* **1965**, *65*, 247.

(5) Akiya, S.; Tejima, S. *J. Pharm. Soc. Jpn.* **1952**, *72*, 1574, 1577, 1580; *Chem. Abstr.* **1953**, *47*, 9275g.

(6) A preliminary account was presented at the 110th Annual Meeting of the Pharmaceutical Society of Japan: Hatano, K.; Uno, T.; Kato, K.; Takeda, T.; Chiba, T.; Tejima, S. Abstract 21C 10-00, Sapporo, Japan, 1990.

0002-7863/91/1513-3069$02.50/0